Critical Temperature of Chiral Symmetry Restoration for Quark Matter with a Chiral Chemical Potential

M. Ruggieri

College of Physics, University of Chinese Academy of Sciences, Yuquanlu 19A, Beijing 100049, China.

E-mail: marco.ruggieri@ucas.ac.cn

G. X. Peng

College of Physics, University of Chinese Academy of Sciences, Yuquanlu 19A, Beijing 100049, China.
Theoretical Physics Center for Science Facilities, Institute of High Energy Physics, Beijing 100049, China.

E-mail: gxpeng@ucas.ac.cn

Abstract. In this article we study restoration of chiral symmetry at finite temperature for quark matter with a chiral chemical potential, μ_5, by means of a nonlocal Nambu-Jona-Lasinio model. This model allows to introduce in the simplest way possible a Euclidean momentum, p_E, dependent quark mass function which decays (neglecting logarithms) as $1/p_E^2$ for large p_E, in agreement with asymptotic behaviour expected in QCD in presence of a nonperturbative quark condensate. We focus on the critical temperature for chiral symmetry restoration in the chiral limit, T_c, versus μ_5, as well as on the order of the phase transition. We find that T_c increases with μ_5, and that the transition remains of the second order for the whole range of μ_5 considered.

PACS numbers: 12.38.Aw,12.38.Mh

Keywords: Chiral chemical potential, nonlocal Nambu-Jona-Lasinio model, chiral phase transition.

1. Introduction

Systems with chirality imbalance, namely with a finite chiral density $n_5 = n_R - n_L$ generated by quantum anomalies, have attracted some interest in recent years. In fact gauge field configurations with a finite winding number, Q_W, can change fermions chirality according to the Adler-Bell-Jackiw anomaly [1, 2]. In the context of Quantum Chromodynamics (QCD) such nontrivial gauge field configurations with $Q_W \neq 0$ are instantons and sphalerons, the latter being produced copiously at high

temperature [3, 4]. The large number of sphaleron transitions in high temperature quark-gluon plasma phase of QCD suggested the possibility that net chirality due to quarks interacting with sphalerons, in combination with the magnetic field produced in high energy collisions, might lead to a charge separation phenonemon named the Chiral Magnetic Effect (CME) [5, 6]. Since the first articles about the CME, the interest for the study of a medium with a net chirality spread from QCD to hydrodynamics and condensed matter systems [7, 8, 9, 10, 11, 12, 13, 14, 15, 16, 17, 18, 19, 20, 21, 22].

In order to describe systems with finite chirality in thermodynamical equilibrium, it is customary to introduce the chiral chemical potential, μ_5, which is conjugated to the n_5, see [23, 24, 25, 26, 27, 28, 29, 30, 31, 32, 33, 34, 35, 36, 37, 38, 39] and references therein. Because of quantum anomaly as well as of chirality changing processes, n_5 is not a strictly conserved quantity hence the concept of μ_5 might sound ambiguous; however, naming τ the typical time scale in which chirality changing processes take place, it can be assumed that $\mu_5 \neq 0$ describes a system in thermodynamical equilibrium with a fixed value of n_5 on a time scale much larger than τ. For example in the quark-gluon plasma phase of QCD chirality changing processes have been studied in [40] where it has been found that $\tau \simeq 50 \div 140$ fm/c in the temperature range $T \simeq 225 \div 500$ MeV.

An interesting problem in the context of QCD is the study of chiral symmetry restoration at finite temperature and $\mu_5 \neq 0$. Some previous calculations based on chiral models predicted T_c, the critical temperature for chiral symmetry restoration, to decrease with μ_5 [24, 25, 26, 27, 28]. On the other hand, recent lattice data have shown that critical temperature increases with μ_5 [30, 31], in agreement with results obtained by solving Schwinger-Dyson equations at finite μ_5 [34, 35].

In this article we study chiral symmetry restoration at finite temperature with $\mu_5 \neq 0$, within a Nambu-Jona-Lasinio (NJL) model [41, 42, 43, 44] with a nonlocal interaction kernel [45, 46, 47, 48, 49, 50, 51] which is built in agreement with the current-current quark interactions in the Instanton Liquid Model of QCD vacuum [52]. We use a nonlocal interaction kernel to mimick the ultraviolet behaviour of the constituent quark mass in QCD [53]. We work in the chiral limit which allows to define mathematically the critical temperature as the zero of the second order Ginzburg-Landau (GL) coefficient. The main result of our study is that the critical temperature increases with μ_5 for all the nonlocal kernels used in actual calculations. Moreover, we discuss the order of the chiral phase transition at finite μ_5: we find that although the chiral chemical potential makes the phase transition sharper, it remains of the second order in the range of μ_5 studied, that is for μ_5 up to $O(1)$ GeV. Both $T_c(\mu_5)$ and the absence of a critical endpoint are in agreement with the most recent Lattice results mentioned above.

The plan of the Article is as follows. In Section II we briefly describe the nonlocal NJL model we use in our calculation, presenting the several choices we do for the running dependent mass. In Section III we perform a small μ_5 computation of the second GL coefficient in the free energy. In Section IV we relax the small μ_5 approximation and compute the critical temperature for chiral symmetry restoration as a function of μ_5, as well as determine the order of the phase transition. Finally in Section V we draw our

conclusions.

2. NJL model with momentum dependent quark mass function

In this Section we describe the model we use to compute the critical line for chiral symmetry restoration in the $T - \mu_5$ plane. We use a Nambu-Jona-Lasinio (NJL) model [41, 42] (see [43, 44] for reviews) with a nonlocal interaction kernel inspired by the Instanton Liquid picture of the QCD vacuum [47, 45, 46, 48, 49] which has the advantage to introduce in the simplest way possible a Euclidean momentum dependent quark mass function in agreement with QCD [53, 54]. The action of the model is given by

$$S = \int d^4x \left(\mathcal{L}_0 + \mathcal{L}_4\right), \tag{1}$$

where $\mathcal{L}_0$ is the lagrangian density of free massless quarks with a chiral chemical potential, namely

$$\mathcal{L}_0 = \bar{\psi}\left(i\partial^\mu\gamma_\mu + \mu_5\bar{\psi}\gamma_0\gamma_5\psi\right)\psi, \tag{2}$$

with ψ being a quark field with Dirac, color and flavor indices. In this equation μ_5 is the chiral chemical potential, and its conjugated quantity is the chiral charge density, $n_5 \equiv n_R - n_L$: a finite μ_5 induces a chiral density in the system, and in general the relation between n_5 and μ_5 has to be computed numerically within some model, see for example [25, 26].

In Eq.(1) $\mathcal{L}_4$ corresponds to the interaction term that in compact form can be written as

$$\mathcal{L}_4 = G\left[j_s(x)j_s(x) + j_{ps}(x)j_{ps}(x)\right], \tag{3}$$

where

$$j_s(x) = \int d^4y d^4z F^\star(y-x)F(z-x)\bar{\psi}(y)\psi(z), \tag{4}$$

$$j_{ps}(x) = \int d^4y d^4z F^\star(y-x)F(z-x)\bar{\psi}(y)i\gamma_5\boldsymbol{\tau}\psi(z), \tag{5}$$

correspond to scalar and pseudoscalar currents respectively. The interaction term in Eq. (3) is formally equivalent to a local NJL interaction,

$$\mathcal{L}_4 = G\left[(\bar{\Psi}(x)\Psi(x))^2 + (\bar{\Psi}(x)i\gamma_5\boldsymbol{\tau}\Psi(x))^2\right], \tag{6}$$

written in terms of the dressed quark fields

$$\Psi(x) \equiv \int d^4y F(y-x)\psi(y). \tag{7}$$

In this study we assume chiral symmetry is spontaneously broken by the nonvanishing expectation value of the dressed quark field operator

$$\sigma \equiv G\langle\bar{\Psi}(x)\Psi(x)\rangle \neq 0, \tag{8}$$

hence neglecting pion condensates. Working at finite temperature T the action in momentum space and in finite quantization volume V can be written as

$$S = -\beta V \frac{\sigma^2}{G} + \int \frac{d^4p}{(2\pi)^4} \bar{\psi}(p) \left[\gamma^\mu p_\mu - M(p) + \mu_5 \gamma_0 \gamma_5\right] \psi(p), \tag{9}$$

with $\beta = 1/T$. In the above equation we have introduced the quark mass function

$$M(p) \equiv -2\sigma \mathcal{C}(p), \tag{10}$$

with $\mathcal{C}(p) \equiv F^2(p)$ and $F(p)$ corresponding to the Fourier transform of the form factor F in Eq. (7). The above equation is formally in agreement with nonlocal models in which the nonlocality comes from an effective one-gluon exchange picture, see for example [55, 56, 50, 51, 58, 57]. In QCD it is known since long time that quarks develop a constituent quark mass function in presence of spontaneous chiral symmetry breaking [53], which for large values of Euclidean momentum p_E and in the chiral limit behaves like [58]

$$M_{\rm QCD}(p_E^2) = -\frac{4\pi^2 d_m}{3p_E^2} \frac{[\log(\mu^2/\Lambda_{QCD}^2)]^{-d_m}}{[\log(p_E^2/\Lambda_{QCD}^2)]^{1-d_m}} \langle\bar{\psi}\psi\rangle(\mu), \tag{11}$$

where μ is the renormalization point and $\langle\bar{\psi}\psi\rangle(\mu)$ is the chiral condensate at the scale μ used as a parameter in Operator Product Expansion; $d_m = 12/(33 - 2N_f)$ is the anomalous dimension of the current mass which for $N_f = 2$ gives $d_m = 12/27$. The NJL model with a local interaction kernel misses the asymptotic behaviour of the quark mass function, which instead we will show to be important in the context of matter with $n_5 \neq 0$.

In particular we will assume several specific functional forms for $M(p)$ in Eq. (10), which besides log terms are consistent with the ultraviolet behaviour of the same QCD quantity Eq. (11). Equation (11) is valid only in the ultraviolet limit therefore we need to rely on some ansatz to describe the quark mass function at small Euclidean momentum. We assume the form factor

$$\mathcal{C}(p_E^2) = \theta(\Lambda^2 - p_E^2) + \theta(p_E^2 - \Lambda^2) \frac{\Lambda^2 (\log \Lambda^2/\Lambda_{QCD}^2)^\gamma}{p_E^2 (\log p_E^2/\Lambda_{QCD}^2)^\gamma}, \tag{12}$$

where p_E^2 is the Euclidean squared momentum. For the esponent γ in Eq.(12) we consider here three cases: $\gamma = 0$ for its simplicity; $\gamma = 1$, inspired by the large momentum behaviour of the form factor introduced in [55, 56]; finally $\gamma = 1 - d_m$ where d_m corresponds to the anomalous mass dimension, inspired by the quark mass function derived by Politzer [53].

We also consider smooth form factors. In particular we consider a Yukawa-type form factor, namely [50, 51]

$$\mathcal{C}(p_E^2) = \frac{\Lambda^2}{p_E^2 + \Lambda^2}; \tag{13}$$

then we consider a form factor inspired by the Instanton Liquid Model (ILM) of the QCD vacuum, namely [52]

$$\mathcal{C}(p_E^2) = \frac{d^2 p_E^2}{4} \left\{ \frac{d}{dx} [I_0(x) K_0(x) - I_1(x) K_1(x)] \right\}^2, \tag{14}$$

where d corresponds to the typical instanton size $d \approx 0.36$ fm and $x = |p_E|d/2$. Finally we consider a nonlocal kernel used in nonlocal NJL model studies [55, 56], namely

$$\mathcal{C}(p_E^2) = \theta(\Lambda^2 - p_E^2)e^{-p_E^2 d^2/2} + \theta(p_E^2 - \Lambda^2)\frac{\Lambda^2(\log \Lambda^2/\Lambda_{QCD}^2)}{p_E^2(\log p_E^2/\Lambda_{QCD}^2)}e^{-\Lambda^2 d^2/2}, \quad (15)$$

where d corresponds to the instanton size used in Eq. (14) and $\Lambda = O(1)$ GeV. Equation (15) offers a smooth version of the form factor in Eq. (12) with $\gamma = 1$.

In this article we use imaginary time formalism to deal with finite temperature calculations, thus we introduce $p_0 = ip_4 = i\omega_n$ with $\omega_n = \pi T(2n+1)$ being the fermionic Matsubara frequency. The thermodynamic potential per unit volume in the mean field approximation is then given by

$$\Omega = \frac{\sigma^2}{G} - T\sum_n \int \frac{d^3\boldsymbol{p}}{(2\pi)^3}\mathtt{Tr}\log\beta S^{-1}(\omega_n, \boldsymbol{p}), \quad (16)$$

where the inverse fermion propagator is given by

$$S^{-1}(\omega_n, \boldsymbol{p}) = i\omega_n\gamma_0 - \boldsymbol{\gamma}\cdot\boldsymbol{p} - M(\omega_n, \boldsymbol{p}) + \mu_5\gamma_0\gamma_5. \quad (17)$$

A straigthforward evaluation of the determinant of S^{-1} gives

$$\Omega = \frac{\sigma^2}{G} - N_c N_f T\sum_n \int \frac{d^3\boldsymbol{p}}{(2\pi)^3}\log\beta^4(\omega_n^2 + E_+^2)(\omega_n^2 + E_-^2), \quad (18)$$

where we have defined

$$E_\pm^2 = (p \pm \mu_5)^2 + M(\omega_n, \boldsymbol{p})^2. \quad (19)$$

In this article we will use Eq. (18) to compute the critical line for chiral symmetry restoration with $\mu_5 \neq 0$, by a Ginzburg-Landau (GL) expansion in powers of the condensate σ.

3. Small μ_5 analysis

In this article we are interested to the relation between μ_5 and the critical temperature for a second order phase transition within the non-local model specified by the potential in Eq. (18). Close to the second order phase transition we make a Ginzburg-Landau (GL) expansion of the thermodynamic potential, namely

$$\Omega - \Omega_0 = \frac{\alpha_2}{2}\sigma^2, \quad (20)$$

where the coefficient α_2 depends on temperature and critical temperature is defined as the solution of the equation $\alpha_2(T_c) = 0$; Ω_0 corresponds to the free energy in the phase with $\sigma = 0$ which is just an irrelevant constant and it has been subtracted. In this Section we focus on $\mu_5 \ll T$, hence we expand

$$\alpha_2 = \alpha_{2,0} + \mu_5^2\alpha_{2,2}. \quad (21)$$

The above equation allows to compute, to the lowest order in μ_5/T, the shift of the critical temperature due to μ_5:

$$\delta T_c = -\frac{\alpha_{2,2}(T_c^0)}{a}\mu_5^2, \quad (22)$$

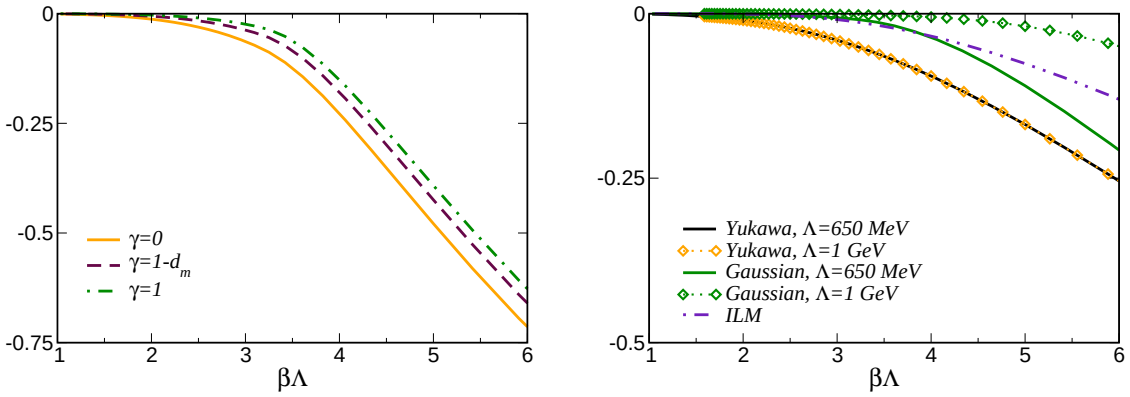

Figure 1. *Left panel.* Coefficient $\alpha_{2,2}$ versus $\beta\Lambda$ obtained within the nonlocal 4D model with the quark mass function specified by Eqs.(12) and(10). *Right panel.* Coefficient $\alpha_{2,2}$ versus $\beta\Lambda$ obtained within the nonlocal 4D model with the quark mass function specified by Yukawa-like form factor Eq.(13), nonlocal NJL form factor in Eq.(15) and Instanton Liquid Model form factor in Eq.(14). For the latter we have introduced a fictitious scale $\Lambda = 650$ MeV on abscissas in order to make comparison with other models easier.

where T_c^0 corresponds to the critical temperature at $\mu_5 = 0$ and $a \equiv d\alpha_{2,0}/dT$ at $T = T_c^0$. The quantity a depends on the specific model used but it is positive by definition because $\alpha_{2,0}$ is negative for $T < T_c$ and positive for $T > T_c$, thus the sign of δT in Eq. 22 is determined only by the sign of $\alpha_{2,2}$. A straightforward computation starting from Eq.(18) shows that

$$\alpha_{2,2} = -4N_c N_f T \sum_n \int \frac{d^3\boldsymbol{p}}{(2\pi)^3} \mathcal{C}^2(\omega_n, \boldsymbol{p}) \frac{2(3\boldsymbol{p}^2 - \omega_n^2)}{(\boldsymbol{p}^2 + \omega_n^2)^3}, \tag{23}$$

where $\mathcal{C}$ is the non local interaction kernel. Once $\alpha_{2,2}$ is known, the critical temperature versus μ_5 can be computed as

$$T_c(\mu_5) = T_c^0 \left[1 - \frac{\alpha_{2,2}(T_c^0)}{aT_c^0}\mu_5^2\right]. \tag{24}$$

In Figure 1 we plot the coefficient $\alpha_{2,2}$ computed by Eq.(23) for the several form factors described in Section 2. For all the models of p_E-dependent quark mass functions we find that $\alpha_{2,2} < 0$, and because of Eq.(24) this implies μ_5 tends to increase the critical temperature for chiral symmetry restoration within the model at hand. This is different from what is obtained within local models in which critical temperature has been found to decrease with μ_5, with the exception of [23] where renormalization has been used to treat the divergent vacuum term.

4. The critical line within Ginzburg-Landau expansion

In this Section we compute the critical line for chiral symmetry restoration as a function of the chiral chemical potential, within a Ginzburg-Landau (GL) expansion of the thermodynamic potential in Eq.(18). In this Section we do not rely on a

small μ_5 expansion as we have done in the previous Section, and we limit ourselves to compute numerically the relevant GL coefficients from which we extract both the critical temperature and the order of the phase transition.

Close to a second order phase transition we can write Eq.(18) as

$$\Omega - \Omega_0 = \frac{\alpha_2}{2}\sigma^2 + \frac{\alpha_4}{4}\sigma^4 + O(\sigma^6), \tag{25}$$

where we have subtracted the thermodynamic potential at $\sigma = 0$, namely Ω_0; α_2 and α_4 can be computed by taking the derivatives of Ω with respect to σ at $\sigma = 0$. We find

$$\begin{aligned}\alpha_2 = \frac{2}{G} - N_c N_f T \sum_n \int \frac{d^3\boldsymbol{p}}{(2\pi)^3} \mathcal{C}^2(\omega_n, \boldsymbol{p}) \\ \times \frac{16(\boldsymbol{p}^2 + \omega_n^2 + \mu_5^2)}{[\omega_n^2 + (p-\mu_5)^2][\omega_n^2 + (p+\mu_5)^2]},\end{aligned} \tag{26}$$

and

$$\begin{aligned}\alpha_4 = & - N_c N_f T \sum_n \int \frac{d^3\boldsymbol{p}}{(2\pi)^3} \mathcal{C}^4(\omega_n, \boldsymbol{p}) \\ & \frac{-384[\boldsymbol{p}^4 + 2\boldsymbol{p}^2(\omega_n^2 + 3\mu_5^2) + (\mu_5^2 + \omega_n^2)^2]}{[\omega_n^2 + (p-\mu_5)^2]^2[\omega_n^2 + (p+\mu_5)^2]^2}.\end{aligned} \tag{27}$$

The nontrivial solution of gap equation, $\partial\Omega/\partial\sigma = 0$, for $T \leq T_c$ is given by

$$\sigma^2(T, \mu_5) = -\frac{\alpha_2(T, \mu_5)}{\alpha_4(T, \mu_5)}, \tag{28}$$

and the critical temperature is defined by the condition $\alpha_2(T, \mu_5) = 0$.

In the upper panel of Fig. 2 we plot the coefficient α_2 in units of the parameter Λ^2 as a function of temperature, for three different values of μ_5. For each value of μ_5 the critical temperature T_c corresponds to $\alpha_2(T_c) = 0$. We show data for the nonlocal model with mass function given by Eqs. (12) and (10) with $\gamma = 0$ and $\Lambda = 900$ MeV; for other models we obtain qualitatively the same results. We notice that, in agreement with the small μ_5 analysis shown in the previous Section, increasing μ_5 results in an increasing critical temperature. We also notice that the slope of α_2 at $T = T_c$ increases with μ_5. Together with the behaviour of α_4 discussed below, this is a signature of the phase transition becoming sharper with μ_5.

In the middle panel of Fig. 2 we plot the coefficient α_4 versus temperature, for the same values of μ_5 shown in the upper panel of the figure. We notice that for any value of μ_5 the coefficient α_4 decreases in magnitude, but it is always positive at the critical temperature meaning the phase transition is a second order one. We also notice that the magnitude of α_4 at $T = T_c(\mu_5)$ decreases compared to the case $\mu_5 = 0$, implying that the phase transition becomes sharper with increasing μ_5. In fact because of Eq. (28) we can write the solution of the gap equation for $T \approx T_c$ as

$$\sigma^2 = -\frac{1}{\alpha_4(T_c)} \left.\frac{d\alpha_2}{dT}\right|_{T=T_c} (T - T_c) + O[(T - T_c)^2], \tag{29}$$

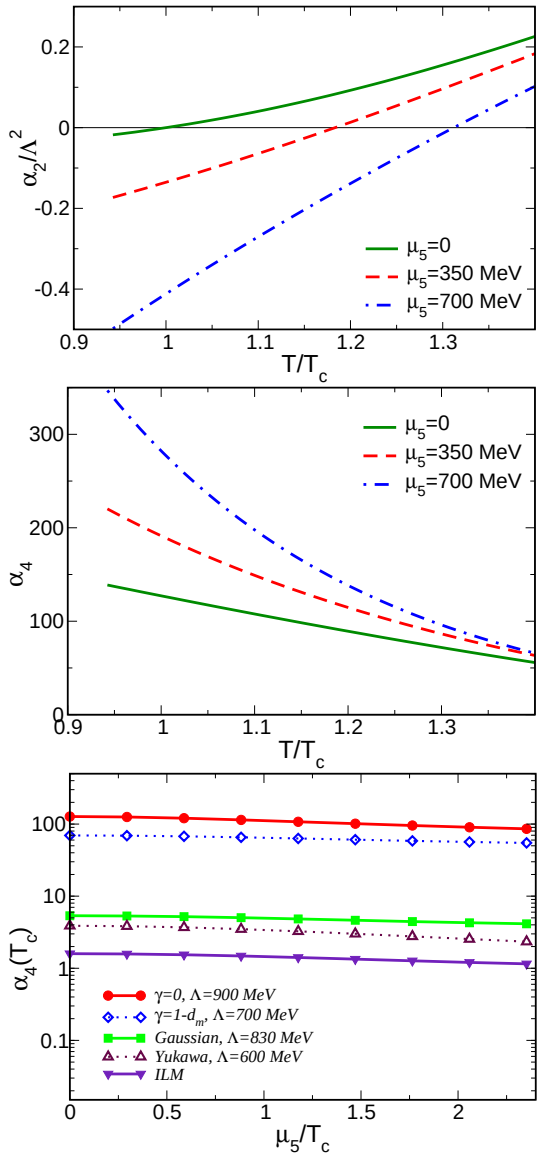

Figure 2. *Upper panel.* Coefficient α_2 in units of the parameter Λ^2 as a function of temperature, for three different values of μ_5. For each value of μ_5 the critical temperature T_c corresponds to $\alpha_2(T_c) = 0$. *Middle panel.* Coefficient α_4 versus temperature, for three different values of μ_5. Upper and middle panels refer to the nonlocal model with mass function given by Eqs. (12) and (10) with $\gamma = 0$ and $\Lambda = 900$ MeV. *Lower panel.* Evolution of the coefficient α_4 computed at $T = T_c(\mu_5)$ versus μ_5 for several models.

then the slope of the condensate at the critical temperature is given by

$$\left.\frac{d\sigma^2}{dT}\right|_{T=T_c} = -\frac{1}{\alpha_4(T_c)}\left.\frac{d\alpha_2}{dT}\right|_{T=T_c}, \tag{30}$$

which becomes larger as we increase μ_5 because α_4 decreases and the slope of α_2 at the critical temperature increases with μ_5. Our conclusion is that within the range of μ_5 explored in our study, we have a firm signal that the phase transition becomes sharper

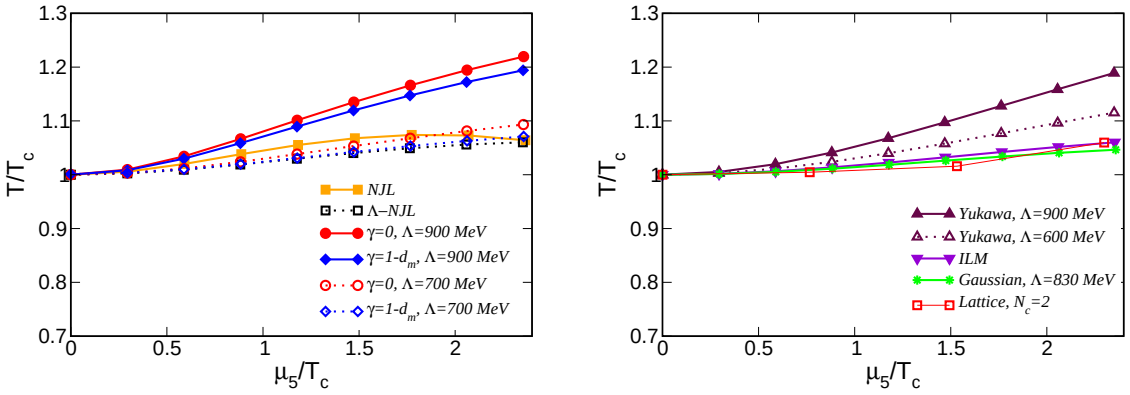

Figure 3. *Left panel.* Critical temperature for chiral symmetry restoration versus μ_5 for several running mass models described in the text. Squares correspond to NJL and $\Lambda-$NJL models with a 4D sharp cutoff $\Lambda = 900$ MeV. Circles correspond to mass function given by Eqs. (12) and (10) with $\gamma = 0$, for two different values of Λ; diamonds correspond to the same mass function with $\gamma = 1-d_m$. *Right panel.* Critical temperature for chiral symmetry restoration versus μ_5 for several running mass models described in the text. Data with triangles pointing upwards correspond to a Yukawa-like form factor in Eq. (13) with two values of Λ. Data denoted by triangles pointing downwards correspond to the Instanton Liquid Model (ILM) form factor in Eq. (14). Stars correspond to the nonlocal form factor in Eq. (15). Lattice data for $N_c = 2$ have been adapted from [31]. In both panels T_c corresponds to critical temperature at $\mu_5 = 0$. The coupling constant G has been tuned in each model at the given value of Λ in order to have $T_c = 170$ MeV.

as μ_5 is increased, but there is no critical endpoint because α_4 does not change sign at the critical temperature. This is in agreement with lattice simulations [30, 31] but it is in disagreement with previous model studies which used a different regularization scheme [24, 26, 25, 27], showing how the existence of the critical point in the phase diagram is very sensitive on the regularization prescription, in fact already noticed in [28]. Finally in the lower panel of Fig. 2 we plot the coefficient α_4 at $T = T_c(\mu_5)$ for several models. We notice that although the numerical value of α_4 strongly depends on the model, we find it is always positive when computed at T_c.

In Fig. 3 we plot the critical temperature versus μ_5 for the nonlocal models described in the text, obtained by the zero of the coefficient α_2. In particular, in the left panel we collect the results for the sharp models described in the text. Circles correspond to mass function given by Eqs. (12) and (10) with $\gamma = 0$, for two different values of Λ; diamonds correspond to the same mass function with $\gamma = 1 - d_m$. In the left panel we have also shown the results for two local NJL models. In particular, we denote by squares the results for a local NJL model with a 4-dimensional sharp cutoff on the vacuum term but no cutoff on the thermal part of the free energy; moreover, empty squares correspond to a model dubbed $\Lambda-$NJL, in which there is a 4D sharp cutoff both on the vacuum and on the thermal contribution to the gap equation. In both cases $\Lambda = 900$ MeV. In the right panel of Fig. 3 we plot the critical temperature for smooth form factors.

In particular data with triangles pointing upwards correspond to a Yukawa-like form factor in Eq. (13) with two values of Λ. Data denoted by triangles pointing downwards correspond to the Instanton Liquid Model (ILM) form factor in Eq. (14). Finally stars correspond to the nonlocal form factor in Eq. (15). In both panels both temperature and chemical potential are measured in units of the critical temperature at $\mu_5 = 0$. In each calculation we have fixed the value of the parameter Λ in the form factor, then we have tuned the NJL coupling constant G in order to obtain $T_c = 170$ MeV at $\mu_5 = 0$ for any model.

The results in Fig. 3 show that for all the nonlocal models studied in this article the critical temperature increases with μ_5, as expected from the small μ_5 analysis of the previous Section. For large values of μ_5 the results shown in Fig. 3 should be not considered very reliable because we have neglected a possible backreaction on the nonlocal interaction kernel due to μ_5. For the case of local models, we find that the $\Lambda-$NJL model still predicts T_c increases with μ_5, at least up to values of μ_5 of the order of Λ. This is in agreement with the previous analysis of [28] where a $\Lambda-$NJL with a 3-dimensional cutoff has been considered. For the NJL model result in Fig. 3 we find that T_c increases with μ_5 for small values of μ_5, then it decreases. We would like to mention that in this case the critical line bends downwards for values of μ_5 considerably smaller than the ultraviolet cutoff, hence the change of the slope of T_c cannot be directly related to the cutoff; we have checked instead that in this case the change of slope in T_c is due to taking into account all the modes in the gap equation at finite temperature rather than cutting them at $p_E = \Lambda$, in agreement with [28].

A detailed comparison with lattice data [30, 31] is premature because those data have not been obtained in the chiral limit; moreover some data on the lattice correspond to $N_c = 2$ QCD while here we consider $N_c = 3$. However we can at least compare the magnitude of the increase of the critical temperature obtained within the nonlocal models and within the lattice simulations. In Fig. 3 we show lattice results for $T_c(\mu_5)$ for $N_c = 2$ adapted from Ref. [31] in which the critical temperature at $\mu_5 = 0$ is $T_c = 195.8 \pm 0.4$ MeV. We find that among the models considered here, the ones with Gaussian ILM form factors, respectively Eqs. (15) and (14), better reproduce the magnitude of the variation of the critical temperature with μ_5.

5. Conclusions

In this article we have presented a model study of the critical temperature of chiral symmetry restoration, T_c, as a function of chiral chemical potential, μ_5. We have used a nonlocal NJL model with several Euclidean interaction kernels, chosen to mimick the constituent quark mass of QCD in the ultraviolet.

We have performed a Ginzburg-Landau expansion of the thermodynamic potential in the vicinity of the second order critical line, and we have focused on the second order coefficient of this expansion, α_2, which allows to determine how the critical temperature runs with μ_5. The results about $T_c(\mu_5)$ are collected in Fig. 3 for the different models.

We have found that within all the nonlocal models used in our study, T_c always increases with μ_5 at least for $\mu_5 \leq \Lambda$ where Λ is the scale at which we match the nonperturbative mass function with its perturbative counterpart, $\Lambda \simeq O(1)$ GeV. We remark that our interaction kernels lack of a backreaction of μ_5, hence our results should be taken with a grain of salt for $\mu_5 = O(1\text{ GeV})$, while they are reliable for smaller values of μ_5.

We have then checked the order of the phase transition by computing the coefficient α_4 of the GL effective potential: we have found that although μ_5 makes the transition sharper because the magnitude of α_4 decreases with μ_5 at T_c, the coefficient never vanishes as it should happen at the critical endpoint. Our conclusion is that there is no trace of a critical endpoint in the phase diagram, at least within the range of μ_5 we have explored in this article, namely for μ_5 approximately up to 1 GeV.

We have also studied how a sharp but covariant 4-dimensional cutoff scheme affects $T_c(\mu_5)$ within the local NJL model: we have found that although for a small range of μ_5 the critical temperature increases, then for μ_5 quite smaller than the cutoff it decreases as it happens in local chiral model calculations with a 3-dimensional cutoff. However, removing by hand the contribution of the thermal excitations with $p_E > \Lambda$ in the gap equation we find $T_c(\mu_5)$ increases also for larger values of μ_5 in agreement with [28].

Finally, we would like to mention that during the very final stage of preparation of the present manuscript, Ref. [59] appeared in which the same problem has been studied and an increasing T_c versus μ_5 has been found, in agreement with the results presented in this article.

Acknowledgments. The authors would like to thank the CAS President's International Fellowship Initiative (Grant No. 2015PM008), and the NSFC projects (11135011 and 11575190). M. R. also acknowledges discussions with M. Frasca.

Appendix A. Analysis of modes contributing to $\alpha_{2,2}$

In this appendix we present a short numerical analysis of the coefficient $\alpha_{2,2}$ defined in Eq. (23), which enlightens the difference between the nonlocal and local models for what concerns $T_c(\mu_5)$ for small values of μ_5. For simplicity, we focus on the form factor given by Eq.(12) with $\gamma = 0$ which allows easier manipulations and a clearer mode separation. A direct computation of $\alpha_{2,2}$ gives

$$\alpha_{2,2} = \mathcal{I}_1 + \mathcal{I}_2 + \mathcal{J}_1 + \mathcal{J}_2, \tag{A.1}$$

where we have split several contributions to the coefficient, depending on the momentum region of quarks and on temperature. We have

- modes with $p_E^2 \leq \Lambda^2$ at $T = 0$:

$$\mathcal{I}_1 = -a_2 \frac{4N_c N_f}{2\pi^2} \log \frac{\Lambda}{m_0}; \tag{A.2}$$

- modes with $p_E^2 > \Lambda^2$ at $T = 0$:

$$\mathcal{I}_2 = -a_1 \frac{4N_c N_f}{2\pi^2}; \tag{A.3}$$

- modes with $p_E^2 \leq \Lambda^2$ at $T > 0$:

$$\mathcal{J}_1 = \frac{4N_cN_f}{2\pi^2}\left[a_2 \log\frac{1}{\beta m_0} + |F(\beta\Lambda)|\right]; \tag{A.4}$$

- modes with $p_E^2 > \Lambda^2$ at $T > 0$:

$$\mathcal{J}_2 = \frac{4N_cN_f}{2\pi^2}|G(\beta\Lambda)|; \tag{A.5}$$

in the above equations $a_1 \approx 0.25$ and $a_2 \approx 0.938$. Moreover we have introduced an infrared cutoff m_0 which appears in the intermediate steps of the computation when the contributions are split; this fictitious cutoff disappears when the sum of the contributions is done, as it is clear from Eqs.(A.4) and (A.2). In the left panel of Fig. (A1) we plot the functions F, G as well as their sum in order to understand the role of the several terms in Eq.(A.1). In particular the modes in Eq.(A.3) come from the high momentum part of the Dirac sea; they are not usually considered in a local model calculation because in that case their contribution is divergent hence it is simply subtracted. We notice that this contribution to $\alpha_{2,2}$ is negative, thus it helps to keep the critical temperature at finite μ_5 higher than that at $\mu_5 = 0$.

We now compare the results of the 4D nonlocal model with those of local models. In particular we introduce a $\Lambda-$NJL model in which we remove all the modes with $p_E^2 > \Lambda^2$; the coefficient will be thus given by

$$\alpha_{2,2}^{\Lambda-\mathrm{NJL}} = -\frac{4N_cN_f}{2\pi^2}\left[a_2 \log\beta\Lambda - |F(\beta\Lambda)|\right]. \tag{A.6}$$

We also introduce a local NJL model in which we remove the ultraviolet modes $p_E^2 > \Lambda^2$ only at $T = 0$, and integrate over all momenta at finite temperature:

$$\alpha_{2,2}^{\mathrm{NJL}} = -\frac{4N_cN_f}{2\pi^2}\left[a_2 \log\beta\Lambda - |F(\infty)|\right], \tag{A.7}$$

where $F(\infty) \equiv \lim_{x\to\infty} F(x)$.

In the right panel of Fig. A1 we plot the coefficient $\alpha_{2,2}$ for the the local NJL model (gren dot-dashed line), the local $\Lambda-$NJL model (maroon dashed line) and the nonlocal model with mass function given by Eqs. (12) and (10) with $\gamma = 0$. For the local models there exists a window of $\beta\Lambda$ in which $\alpha_{2,2} > 0$; on the other hand for the nonlocal model considered here we find $\alpha_{2,2} < 0$ for any value of $\beta\Lambda$. The fact that $\alpha_{2,2}$ can be positive in the local models is due to the absence of the vacuum term in Eq. (A.3) which would give a negative contribution to $\alpha_{2,2}$. The range of $\beta\Lambda$ in which $\alpha_{2,2} > 0$ is quite wide in the case of the NJL model, being shrunk in the case of $\Lambda-$NJL. The results in Fig. A1 suggest that in the local NJL model the slope of $T_c(\mu_5)$ at small μ_5 depends on the ratio T_c/Λ; this is true also in the $\Lambda-$NJL model, but in this case the range of T_c/Λ with a positive $\alpha_{2,2}$ is much smaller.

References

[1] S. L. Adler, Phys. Rev. **177**, 2426 (1969).
[2] J. S. Bell and R. Jackiw, Nuovo Cim. A **60**, 47 (1969).

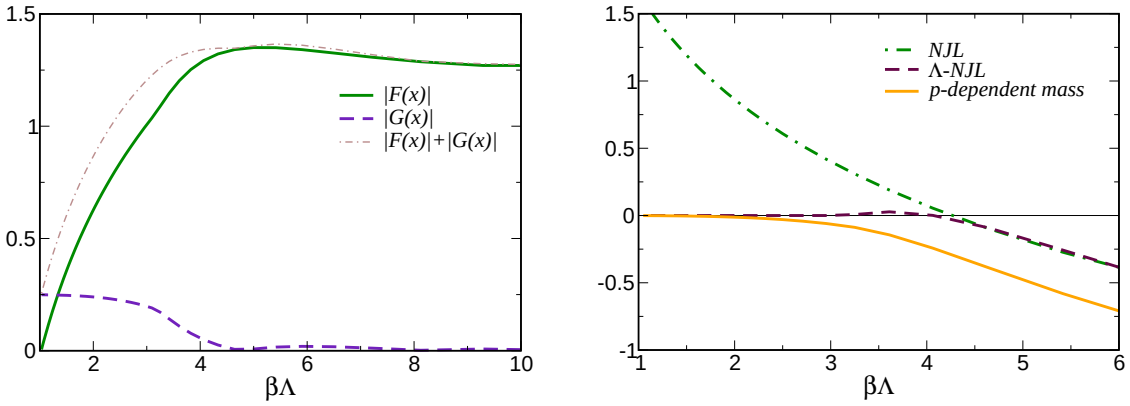

Figure A1. *Left panel.* Functions $F(x)$, $G(x)$ and their sum. *Right panel.* Comparison of the $\alpha_{2,2}$ coefficients for the local NJL model (gren dot-dashed line), the local $\Lambda-$NJL model (maroon dashed line) and the nonlocal model with mass function given by Eqs.(12) and(10) with $\gamma = 0$.

[3] G. D. Moore, hep-ph/0009161.
[4] G. D. Moore and M. Tassler, JHEP **1102**, 105 (2011).
[5] D. E. Kharzeev, L. D. McLerran and H. J. Warringa, Nucl. Phys. A **803**, 227 (2008).
[6] K. Fukushima, D. E. Kharzeev and H. J. Warringa, Phys. Rev. D **78**, 074033 (2008).
[7] D. T. Son and P. Surowka, Phys. Rev. Lett. **103**, 191601 (2009).
[8] N. Banerjee, J. Bhattacharya, S. Bhattacharyya, S. Dutta, R. Loganayagam and P. Surowka, JHEP **1101**, 094 (2011).
[9] K. Landsteiner, E. Megias and F. Pena-Benitez, Phys. Rev. Lett. **107**, 021601 (2011).
[10] D. T. Son and A. R. Zhitnitsky, Phys. Rev. D **70**, 074018 (2004).
[11] M. A. Metlitski and A. R. Zhitnitsky, Phys. Rev. D **72**, 045011 (2005).
[12] D. E. Kharzeev and H. U. Yee, Phys. Rev. D **83**, 085007 (2011).
[13] M. N. Chernodub, JHEP **1601**, 100 (2016).
[14] M. N. Chernodub and M. Zubkov, arXiv:1508.03114 [cond-mat.mes-hall].
[15] M. N. Chernodub, A. Cortijo, A. G. Grushin, K. Landsteiner and M. A. H. Vozmediano, Phys. Rev. B **89**, no. 8, 081407 (2014).
[16] V. Braguta, M. N. Chernodub, K. Landsteiner, M. I. Polikarpov and M. V. Ulybyshev, Phys. Rev. D **88**, 071501 (2013).
[17] Q. Li *et al.*, arXiv:1412.6543 [cond-mat.str-el].
[18] A. V. Sadofyev and M. V. Isachenkov, Phys. Lett. B **697**, 404 (2011).
[19] A. V. Sadofyev, V. I. Shevchenko and V. I. Zakharov, Phys. Rev. D **83**, 105025 (2011).
[20] Z. V. Khaidukov, V. P. Kirilin, A. V. Sadofyev and V. I. Zakharov, arXiv:1307.0138 [hep-th].
[21] V. P. Kirilin, A. V. Sadofyev and V. I. Zakharov, arXiv:1312.0895 [hep-th].
[22] A. Avdoshkin, V. P. Kirilin, A. V. Sadofyev and V. I. Zakharov, Phys. Lett. B **755**, 1 (2016).
[23] M. Ruggieri and G. X. Peng, arXiv:1602.03651 [hep-ph].
[24] R. Gatto and M. Ruggieri, Phys. Rev. D **85**, 054013 (2012).
[25] K. Fukushima, M. Ruggieri and R. Gatto, Phys. Rev. D **81**, 114031 (2010).
[26] M. N. Chernodub and A. S. Nedelin, Phys. Rev. D **83**, 105008 (2011).
[27] M. Ruggieri, Phys. Rev. D **84**, 014011 (2011).
[28] L. Yu, H. Liu and M. Huang, arXiv:1511.03073 [hep-ph].
[29] L. Yu, J. Van Doorsselaere and M. Huang, Phys. Rev. D **91**, no. 7, 074011 (2015).
[30] V. V. Braguta, E.-M. Ilgenfritz, A. Y. Kotov, B. Petersson and S. A. Skinderev, arXiv:1512.05873 [hep-lat].

[31] V. V. Braguta, V. A. Goy, E.-M. Ilgenfritz, A. Y. Kotov, A. V. Molochkov, M. Muller-Preussker and B. Petersson, JHEP **1506**, 094 (2015).
[32] V. V. Braguta and A. Y. Kotov, arXiv:1601.04957 [hep-th].
[33] M. Hanada and N. Yamamoto, PoS LATTICE **2011**, 221 (2011) [arXiv:1111.3391 [hep-lat]].
[34] S. S. Xu, Z. F. Cui, B. Wang, Y. M. Shi, Y. C. Yang and H. S. Zong, Phys. Rev. D **91**, no. 5, 056003 (2015).
[35] B. Wang, Y. L. Wang, Z. F. Cui and H. S. Zong, Phys. Rev. D **91**, no. 3, 034017 (2015).
[36] D. Ebert, T. G. Khunjua, K. G. Klimenko and V. C. Zhukovsky, Phys. Rev. D **93**, no. 10, 105022 (2016).
[37] S. S. Afonin, A. A. Andrianov and D. Espriu, Phys. Lett. B **745**, 52 (2015).
[38] A. A. Andrianov, D. Espriu and X. Planells, Eur. Phys. J. C **73**, no. 1, 2294 (2013).
[39] X. Planells, A. A. Andrianov, V. A. Andrianov and D. Espriu, PoS QFTHEP **2013**, 049 (2013) [arXiv:1310.4434 [hep-ph]].
[40] C. Manuel and J. M. Torres-Rincon, Phys. Rev. D **92**, no. 7, 074018 (2015).
[41] Y. Nambu and G. Jona-Lasinio, Phys. Rev. **122**, 345 (1961).
[42] Y. Nambu and G. Jona-Lasinio, Phys. Rev. **124**, 246 (1961).
[43] S. P. Klevansky, Rev. Mod. Phys. **64**, 649 (1992).
[44] T. Hatsuda and T. Kunihiro, Phys. Rept. **247**, 221 (1994).
[45] S. M. Schmidt, D. Blaschke and Y. L. Kalinovsky, Phys. Rev. C **50**, 435 (1994).
[46] R. D. Bowler and M. C. Birse, Nucl. Phys. A **582**, 655 (1995).
[47] R. S. Plant and M. C. Birse, Nucl. Phys. A **628**, 607 (1998).
[48] D. Blaschke, G. Burau, Y. L. Kalinovsky, P. Maris and P. C. Tandy, Int. J. Mod. Phys. A **16**, 2267 (2001).
[49] D. Gomez Dumm, D. B. Blaschke, A. G. Grunfeld and N. N. Scoccola, Phys. Rev. D **73**, 114019 (2006).
[50] M. Frasca, Phys. Rev. C **84**, 055208 (2011).
[51] M. Frasca, JHEP **1311**, 099 (2013).
[52] T. Schfer and E. V. Shuryak, Rev. Mod. Phys. **70**, 323 (1998).
[53] H. D. Politzer, Nucl. Phys. B **117**, 397 (1976).
[54] J. Gasser and H. Leutwyler, Phys. Rept. **87**, 77 (1982).
[55] T. Hell, S. Roessner, M. Cristoforetti and W. Weise, Phys. Rev. D **79**, 014022 (2009).
[56] T. Hell, S. Rossner, M. Cristoforetti and W. Weise, Phys. Rev. D **81**, 074034 (2010).
[57] K. Langfeld and C. Kettner, Mod. Phys. Lett. A **11**, 1331 (1996).
[58] K. Langfeld, C. Kettner and H. Reinhardt, Nucl. Phys. A **608**, 331 (1996).
[59] M. Frasca, arXiv:1602.04654 [hep-ph].